Journal Pre-proofs

Injectable Thermoresponsive Gels Offer Sustained Dual Release of Bupivacaine Hydrochloride and Ketorolac Tromethamine For Up To Two Weeks

Hani Abdeltawab, Darren Svirskis, Ben J Boyd, Andrew Hill, Manisha Sharma

PII: S0378-5173(21)00553-6
DOI: https://doi.org/10.1016/j.ijpharm.2021.120748
Reference: IJP 120748

To appear in: *International Journal of Pharmaceutics*

Received Date: 12 April 2021
Revised Date: 23 May 2021
Accepted Date: 24 May 2021

Please cite this article as: H. Abdeltawab, D. Svirskis, B.J. Boyd, A. Hill, M. Sharma, Injectable Thermoresponsive Gels Offer Sustained Dual Release of Bupivacaine Hydrochloride and Ketorolac Tromethamine For Up To Two Weeks, *International Journal of Pharmaceutics* (2021), doi: https://doi.org/10.1016/j.ijpharm.2021.120748

Injectable Thermoresponsive Gels Offer Sustained Dual Release of Bupivacaine Hydrochloride and Ketorolac Tromethamine For Up To Two Weeks

Hani Abdeltawab[1], Darren Svirskis[1], Ben J Boyd[2], Andrew Hill[3], Manisha Sharma[1*]

[1] School of Pharmacy, Faculty of Medical & Health Sciences, The University of Auckland, New Zealand.

[2] Drug Delivery, Disposition and Dynamics and ARC Centre of Excellence in Convergent Bio-Nano Science and Technology, Monash Institute of Pharmaceutical Sciences, Monash University (Parkville Campus), 381 Royal Parade, Parkville, VIC 3052, Australia.

[3] Department of Surgery, School of Medicine, The University of Auckland, Middlemore Hospital, Auckland, New Zealand

*Correspondence:

Dr. Manisha Sharma

Tel.: + 64 9 373 7599 Ext 81830

Fax: +64 9 367 7192

E-mail address: manisha.sharma@auckland.ac.nz

Postal address: School of Pharmacy

Faculty of Medical and Health Sciences

University of Auckland

Private Bag 92019

Auckland

New Zealand

Abstract

Bupivacaine and ketorolac are commonly used in combination to reduce perioperative pain. This study aimed to develop and characterize an injectable system that offers simultaneous and prolonged release of bupivacaine and ketorolac. Formulations were prepared using poloxamer 407 with increasing concentrations of poloxamer 188 and sodium chloride. Small angle X-ray scattering (SAXS) experiments demonstrated that the poloxamers form gels with a cubic lattice arrangement regardless of the matrix composition, whereas the system porosity is driven by poloxamers concentration. Drug loading slightly reduced the intermicellar spacing. Fourier transform infrared spectroscopy and thermal analysis suggested electrostatic interactions between the loaded drugs and poloxamers. Mechanical and rheological studies confirmed the formulations exhibit Newtonian-like flow at room temperature followed by a transition to a viscous gel at body temperature. Importantly, the developed formulations demonstrated steady and sustained release of both bupivacaine and ketorolac over two weeks. Sodium chloride reduced the initial burst release over the first six hours for BH, from 8.6 ± 0.18% to 1.6 ± 0.11%, and KT, from 7.7 ± 0.27% to 1.5 ± 0.10%. Hence, poloxamer-based thermoresponsive gelling systems are promising delivery platforms for the sustained delivery of bupivacaine and ketorolac, with potential clinical benefits for managing perioperative pain.

Keywords

Poloxamers; Bupivacaine; Ketorolac; Pain; Small Angle X-ray Scattering (SAXS); Sustained release

Highlights

- Bupivacaine and ketorolac are chemically compatible with poloxamers
- Micelles aggregate to form a gel with a cubic lattice arrangement
- Sol-to-gel transition temperature can be tailored by adjusting PPO/PEO ratio
- Gel porosity and drug diffusion rate can be altered by modifying matrix concentration
- Inclusion of sodium chloride is a promising strategy to limit initial burst release

1. Introduction

In clinical practice, multimodal analgesia is commonly employed for the management of intense pain, such as perioperative pain (1). This approach involves administering drug combinations, each drug with a different mechanism of action (1). A combination of the local anesthetic bupivacaine hydrochloride (BH) and the anti-inflammatory agent ketorolac tromethamine (KT) has previously been demonstrated to effectively control perioperative pain, reduce hospital stays, speed patient recovery and reduce opioid requirements (2–4). Yet, the therapeutic benefits of this approach are strongly limited by the short half-lives and the rapid elimination of BH and KT from the site of administration (5,6). There are no marketed BH/KT combination products, therefore BH/KT parenteral admixtures are generally extemporaneously compounded in the hospitals prior to administration, limiting availability and exposing the patient to potential risks such as errors in dosing (7). Furthermore, the literature lacks data about the compatibility of their admixtures, exposing the patient to potential harm. Therefore, an injectable sustained release formulation that offers prolonged local delivery of both BH and KT simultaneously has potential clinical benefits for the management of perioperative pain.

Bupivacaine is a long-acting local anesthetic (Figure 1A), commonly used for the management of perioperative pain (8). Pharmacologically, BH interrupts signal conduction by inhibiting sodium influx and, therefore, hindering the generation and propagation of action potentials in nerves (8). The elimination half-life of BH varies depending on the administration site: 0.65 ± 0.2 hours following intravenous administration and 2.8 ± 0.5 hours after epidural administration (5). BH is a white crystalline powder that is freely soluble in water (50 mg/ml) (9,10). Nonetheless, BH exhibits pH dependent solubility, which decreases to 0.15 mg/ml, with a pH rise above 8 (11). Ketorolac (Figure 1B) is a potent nonsteroidal anti-inflammatory drug (NSAID) with 50-fold greater analgesia than naproxen and analgesic effects comparable to opioids such as morphine and oxymorphone (12,13). Pharmacologically, KT inhibits both cyclooxygenase; COX-1 and COX-2 enzymes, and its elimination half-life is 4.5 hours. KT is an off-white crystalline powder that is highly water soluble (56.5 mg/ml) and exhibits limited aqueous solubility (0.86 mg/ml) above pH 9 (14–16). Of note, KT administered systemically is associated with severe adverse reactions such as nephrotoxicity, gastrointestinal ulcers and bleeding (17). Therefore, localized delivery of KT is desirable to reduce these systemic side effects.

Poloxamers (Figure 1C) are Food and Drug Administration (FDA) approved thermoresponsive triblock copolymers, composed of repeated units of polyethylene oxide (PEO) and

polypropylene oxide (PPO) (18). Their concentrated solutions are injectable liquids at room temperature yet form a highly viscous gel at the physiological temperature, with a potential to serve as a slow-release drug depot at the site of administration (19,20). Poloxamer-based *in-situ* gels are biocompatible and bioerodible systems and are widely investigated for drug delivery. The employment of poloxamers for the delivery of anesthesia/analgesia is limited by the initial burst release of the loaded drug and the short duration of action (21–24). Extended drug delivery from poloxamers can be achieved by adjusting the hydrophobicity/hydrophilicity (PPO/PEO) of the poloxamer composition. Interestingly, the inclusion of sodium chloride (NaCl) into poloxamer mixtures enhances the hydrophobic interactions between poloxamers chains, facilitating a rapid sol-to-gel transition (18), which has been suggested to limit the initial burst release of the loaded drugs.

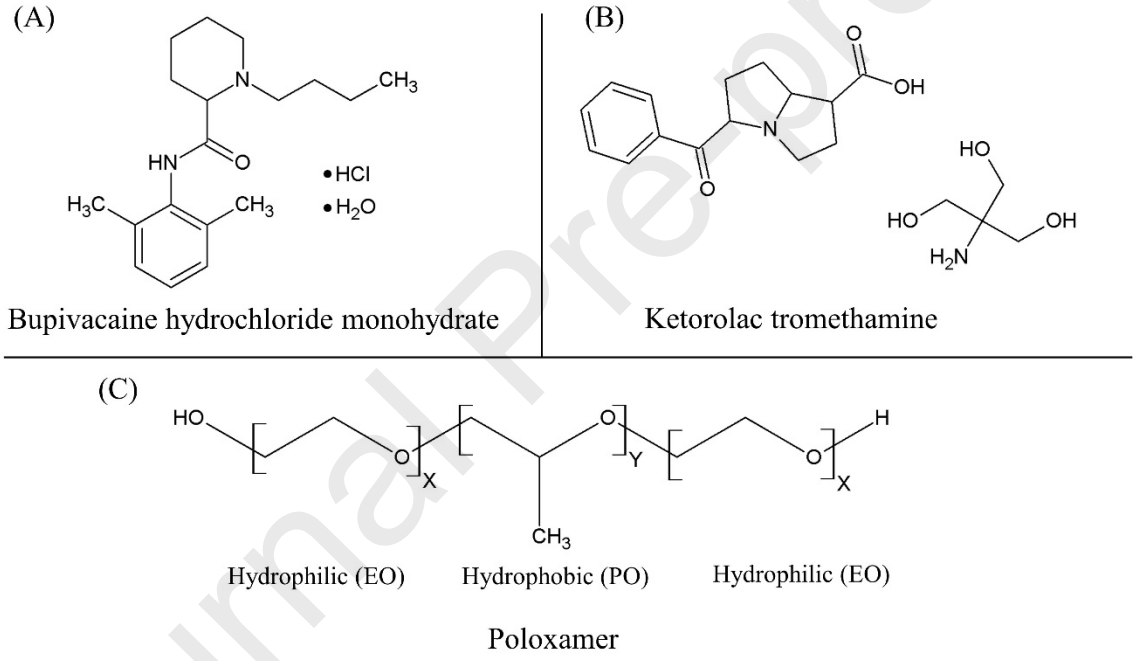

Figure 1:Chemical structures of (A) bupivacaine hydrochloride monohydrate, (B) ketorolac tromethamine and (C) poloxamers, where X and Y are the average numbers of repeating units of each blockchain (for poloxamer 188 X is 76 and Y is 29 (EO/PO = 5.24), while for poloxamer 407 X is 100, while Y is 65 (EO/PO = 3.07)).

This work, for the first time, describes thermoresponsive *in-situ* gels based on poloxamers for the sustained delivery of both BH and KT. The role of the PPO/PEO ratio, poloxamer concentration and the inclusion of a salt additive, to achieve sustained release for an extended duration was studied. In addition, the relationships between gel supramolecular arrangement, system porosity and *in vitro* release profiles were investigated. Furthermore, this manuscript offers a simple and feasible approach to overcome the initial burst drug release that is commonly reported from poloxamers based in-situ gels (21–24).

2. Materials and Methods

2.1. Materials

Bupivacaine hydrochloride monohydrate (BH) and ketorolac tromethamine (KT) were purchased from Jai Radhe Sales (India). Poloxamer 407 (P407), poloxamer 188 (P188) and phosphate-buffered saline (PBS) tablets were purchased from (Sigma-Aldrich, USA). Water was obtained from a Milli-Q water purification system (Millipore, Darmstadt, Germany) with an 18 MΩ.cm resistivity. All other solvents and reagents used were of analytical grade.

2.2. Preparation of *in-situ* gel formulations

Thermoresponsive *in-situ* gelling systems were prepared as previously described (24). Briefly, predetermined weights of P407 and P188 were dissolved in specified amounts of water at 4℃, by stirring overnight. Formulations were prepared with 23% w/w P407 alone, as well as formulations containing P188 at 5.5 or 11% w/w. Based on sol-to-gel transition temperature, a base formulation (F3) was selected and blended with sodium chloride (0.4% w/w NaCl). The mixture was stirred at 4℃ until complete dissolution. All formulations were loaded with both BH (1% w/w) and KT (1% w/w) and stirred until complete dissolution of drugs. The composition of developed formulations is shown in Table 1.

2.3. Sol-to-gel transition

The sol-to-gel transition temperature of BH/KT loaded formulations was determined using AR-G2 rheometer (TA instruments, Melbourne, Australia) equipped with a temperature-controlled Peltier plate and a stainless steel parallel plate geometry (40 mm), as described by Svirskis *et al.* with modification (24). The formulation (1.5 ml) was sandwiched between the parallel plate and the Peltier plate and subjected to a temperature ramp in the range of 10 to 40℃ at a rate of 4°C/min. The viscosity of the formulations was plotted as a function of the temperature. The sol-to-gel transition temperature was identified as the temperature at which the sample demonstrated a sharp increase in viscosity (25).

The reversible sol-to-gel transition was studied by subjecting the formulations to subsequent heating (10 to 40°C) and cooling cycles (40 to 10℃) at a rate of 4℃/min. Changes in viscosity were determined as a function of temperature.

2.4. Small-angle X-ray scattering (SAXS) analysis

Small angle X-ray scattering studies were conducted on the SAXS/WAXS beamline at the Australian Synchrotron, ANSTO, Melbourne (26). Samples were loaded into glass capillaries (1.5 mm diameter, Charles Supper, Natick, MA) at 4°C using a syringe and needle. Capillaries

were loaded into a temperature-controlled capillary holder, mounted in the path of the X-ray beam (photon energy: 13 keV), and measurements were taken with a 1 s acquisition time. Temperature was set via a water bath with a thermocouple placed in the capillary holder to accurately record sample temperature. Temperature was equilibrated for 10 min before acquisition, and acquisitions were made at approximately 5°C intervals from 5-50°C. A Pilatus 1 M (170 mm × 170 mm) detector, located approximately 900 mm from the sample position, was used to generate two-dimensional SAXS patterns, which were reduced to scattering functions plotted as intensity (I) versus scattering vector (q) using Scatterbrain software version 2.71 developed in-house. Lattice parameters were calculated using known relationships relating peak positions to lattice dimensions (27).

2.5. Chemical compatibility/interaction of BH, KT and poloxamers

2.5.1. Fourier Transform Infra-Red Spectroscopy (FTIR)

To probe intermolecular interactions between formulation components, a Bruker Tensor 37 FTIR spectrophotometer (Bruker Tensor 37, Germany) equipped with OPUS 6.5 software was used. Solutions of poloxamers (188 and 407, 1:4), BH, BH/poloxamers (1:1 mixture), KT, KT/poloxamers (1:1 mixture), poloxamers/NaCl mixture and BH/KT (1:1 mixture) were prepared in water, freeze-dried, and the spectra of the freeze-dried powders were recorded. Measurements were performed in attenuated total reflectance (ATR) mode using a diamond crystal, over a wavenumber range of 400–4000 cm^{-1}. Data were collected with 1 cm^{-1} resolution, taking 64 scans per sample.

2.5.2. Thermal analysis

The thermal behavior of the developed formulations was studied using differential scanning calorimetry (DSC), TA instruments (USA) Q-200 DSC apparatus. Briefly, solutions of poloxamers (P188 and P407, 1:4), BH, BH/poloxamers (1:1 mixture), KT, KT/poloxamers (1:1 mixture), poloxamers/ NaCl mixture and BH/KT (1:1 mixture) were prepared in water and freeze-dried. Samples (3-10 mg) were transferred into standard aluminum pans, and the sealed pans were subjected to heating over a temperature range of 0 - 300℃ at a rate of 10℃/min. An empty pan was used as a reference, and a plot of heat flux against temperature was constructed for each sample.

2.6. Mechanical properties

2.6.1. Gel strength

The gel strength was determined via texture analysis (TA.XT Stable Microsystems, Surrey, UK). The test was carried out, as described by Sharma *et al*. with modifications (23). Briefly, a sample (15 ml) was transferred into a 20 ml cylindrical glass vial (25 mm internal diameter) and kept at 37℃ in a temperature-controlled Peltier cabinet for 30 min to achieve complete gelation. A Delrin cylinder probe (10 mm) was allowed to pass through the gel at a speed of 1 mm/second to a depth of 5 mm using a trigger force of 5.0 g. Gel strength and hardness were derived from the resultant force-time plot using the Exponent 32 software (28).

2.6.2. Injectability

Injectability studies were done using a universal syringe rig (A/USR) attachment (Stable Microsystems, Surrey, UK), as described by Shavandi *et al.* with modification (29). The formulations were loaded into a 3 ml syringe attached to an 18-gauge needle. The syringe was attached to the syringe rig, and the probe was allowed to compress the syringe plunger to a distance of 20 mm at a speed of 5 mm/second. The maximum force and the total work required to expel the formulation were determined, as described by Qiangnan Zhang *et al*. (30). The maximum force was calculated from the force-time plot as the highest force achieved before the content was expelled. Whereas the total work required for injection was calculated as the total positive area obtained by the force-distance plot as plotted by the texture analyzer Exponent 32 software.

2.7. Rheological properties

The rheological properties were determined using AR-G2 rheometer (TA instruments, Melbourne, Australia) equipped with a temperature-controlled Peltier plate and a stainless-steel parallel plate geometry (40 mm).

2.7.1. Viscosity and flow properties analysis

The flow-ability of the formulations was determined by viscosity measurement as a function of shear rate over the range of 2 - 200 sec^{-1} at 20℃.

2.7.2. Gel linear viscoelastic behavior

To identify the gel linear viscoelastic region, a strain-sweep analysis was performed at 37℃ ± 0.1 and fixed angular frequencies (10 and 100 rad/s) over the strain amplitude range of 0.01 to 15%.

To study the viscoelastic behaviour of the gels, an oscillation sweep was performed at 37℃ ± 0.1 over an angular frequency range of 0.1 to 100 rad/s within the linear viscoelastic region (at

a constant and low strain amplitude of 0.02 Pa), as described by J.Hu *et al*. (31). The changes in storage and loss moduli were determined as a function of angular frequency (31).

2.8. *In vitro* drug release studies

In vitro drug release studies were conducted in flat bottom falcon tubes using PBS (pH 7.4) as release media, under sink conditions (BH and KT concentrations in the release medium was never more than 10% of the saturated concentration), as described by Svirskis *et al.* (24). Briefly, a known amount of each formulation (1 g) was injected into a tube containing 4 ml of PBS (prewarmed to 37℃). The tubes were placed at a rocking shaker and agitated at 10 rpm. The temperature was maintained at 37℃ throughout the study. At specified time intervals, aliquots (50 µL) were withdrawn and replaced by fresh prewarmed PBS to maintain the sink conditions. The aliquots were diluted with appropriate volumes of the mobile phase and analyzed using a high-performance liquid chromatography (HPLC) method, developed and validated in the laboratory. The results were expressed as a percentage cumulative drug release against time. The similarity of BH/KT release profiles among developed formulations was calculated using the similarity factor (f2). To identify the dominant mechanism of drug release, the *in vitro* drug release data was applied to zero order, first order, Higuchi and Hixson-Crowel release kinetics models.

2.9. Statistical analysis of data

All results are represented as mean ± standard deviation (SD), where n = 3. The statistical differences were calculated using one-way analysis of variance (One-way ANOVA), with multiple comparisons to the formulation (F4), and paired t-test. The confidence level of significance was calculated using the software GraphPad Prism 8.2.1 (Graph Pad Software Inc., USA).

3. Results and discussion

3.1. Sol-to-gel transition

Table 1 shows the composition and sol-to-gel transition temperatures of blank and BH/KT loaded formulations. As presented, a direct relationship was observed between P188 concentration and sol-to-gel transition temperature. Formulation (F2) with a lower PPO/PEO ratio, underwent a phase transition at higher temperatures since more energy is required to break down the abundant hydrogen bonds between hydrophilic EO units and water (32). In comparison, formulation F4 easily dehydrated at a significantly lower temperature ($P < 0.0001$), attributed to its relatively higher PPO/PEO ratio. The addition of NaCl in formulation F3NaCl,

significantly reduced the gelation temperature (P <0.005), which has previously been attributed to the salting out effect (33,34). NaCl forms ionic crosslinks with poloxamers, enhancing the hydrophobic interactions between poloxamer molecules, thereby accelerating the phase transition. The addition of 1% w/w BH and KT significantly reduced the phase transition temperature (P <0.005), suggesting an intermolecular interaction with poloxamers. The pH of the drug-loaded formulations ranged from 6.5 to 6.9, considering the pKa of the drugs (BH – 8.15 and KT – 3.5 (11,35)) they are predominately in ionized forms, potentially interacting with the micellar corona and causing a reduction in the phase transition temperature (36,37).

The speed of sol-to-gel phase transition is also critical and governs the initial burst release from poloxamer gels. As evident from Figure 2A, formulations F4 and F3NaCl exhibited a higher gradient in the viscosity curves suggesting faster sol-to-gel transition as compared to F2 and F3. Formulations with faster sol-to-gel transition are likely to have a shorter lag time between injection and gel formation and, thus, will have limited burst release following administration.

In agreement with the literature, all formulations exhibited a reversible phase transition. Yet, a hysteresis in viscosity curves was observed between the heating and cooling cycles (Figure 2B). This could be attributed to the difference in energy transfer (gain and loss) rates between liquid and semi-solid matrices, leading to a difference in the speed of different physical phenomena, such as micellar aggregation and disassembly (38,39).

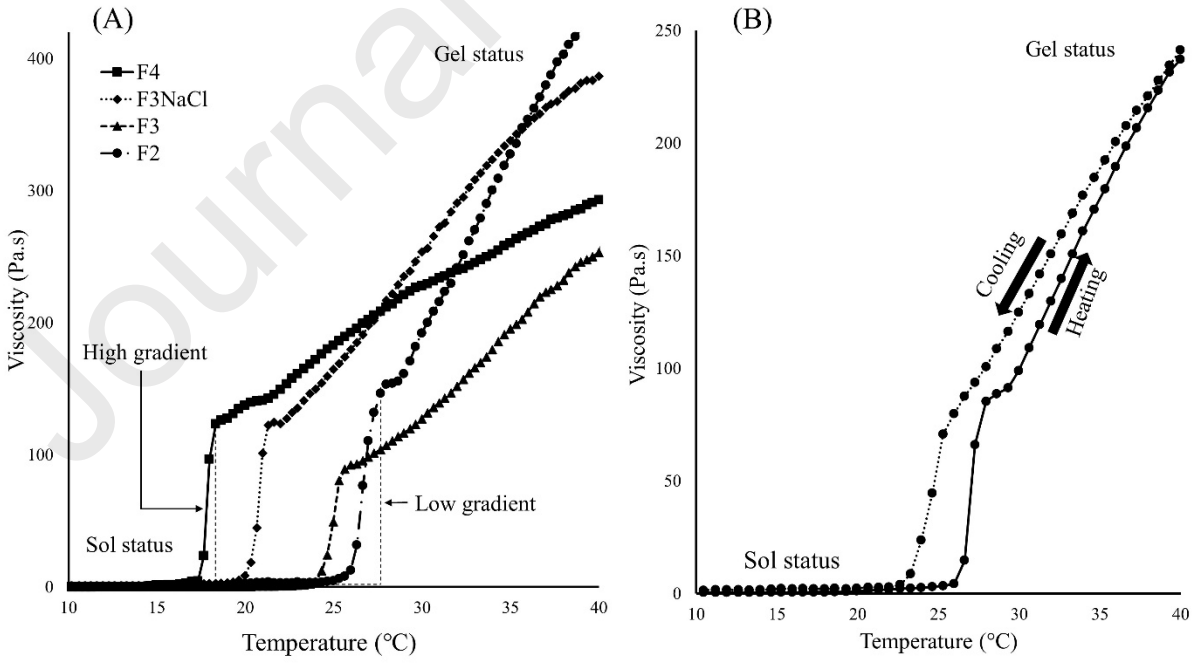

Figure 2: Viscosity changes of BH/KT loaded formulations as a function of temperature; (A) showing the relatively higher gradient of F4 and F3NaCl, suggesting a faster phase transition, and the lower gradient of F3 and

F2, suggesting a slower sol-to-gel transition, and (B) the reversible phase transition of F2 showing a hysteresis between sol-to-gel and gel-to-sol transitions.

Table 1: Composition and sol-to-gel transition temperature of blank and BH/KT loaded formulations, showing the impact of P188, NaCl and drugs (BH/KT) inclusion on the phase transition temperature (n=3 ± s.d.).

Formulation code	P407 (% w/w)	P188 (% w/w)	Water (% w/w)	NaCl (% w/w)	PPO/PEO ratio	Sol-to-gel transition temperature (ºC) Mean ± SD	
						Blank	BH & KT loaded (1% w/w of each)
F2	23	11	66	——	0.28	28.4 ± 0.2	26.6 ± 0.3
F3	23	5.5	71.5	——	0.30	26.6 ± 0.0	24.9 ± 0.5
F4	23	——	77	——	0.33	19.6 ± 0.0	17.9 ± 0.2
F3NaCl	23	5.5	71.5	0.4	0.30	23.6 ± 0.0	20.9 ± 0.3

3.2. SAXS analysis

3.2.1. Micellization and phase transition

SAXS diffraction profiles of BH/KT loaded formulations as a function of temperature are shown in Figure 3. An inverse relationship was observed between the critical micellization temperature (CMT) and concentration of poloxamer; CMT was recorded as 7, 12 and 16.5℃ for F2, F3 and F4, respectively, attributed to the fact that micellization is a concentration-driven process (40,41). The inclusion of NaCl reduced the CMT from 12 to 7°C, attributed to the increased hydrophobic interactions (42,43).

As temperature rises, micellar growth and entanglement occur, causing the system to undergo a disordered to an ordered transition (DOT). In agreement with the rheological data, the SAXS findings denote that the temperature range required to achieve the transition from discrete micellar structures to a packed system is altered by the matrix hydrophobicity and concentration. As presented in Figure 3, F2 exhibited micellization at 7℃ yet maintained the disordered phase up to 22℃, whereas F4 exhibited both micellization and transition at 16.5℃. This could be explained by the differences in PPO/PEO ratios. A formulation that has low ratio of PPO/PEO, such as F2, requires more energy to break down the hydrogen bonds between hydrated PEO blocks and water and achieve micellar entanglement, and vice versa. Likewise, F3NaCl exhibited a transition from disordered to a face-centered cubic arrangement at a lower

temperature (12.5℃) compared to F3 (16.5℃), attributed to its salting out effect and ionic crosslinking between NaCl and poloxamers, facilitating the hydrophobic interaction between micelles (33,34).

The temperature at which all unimers are transferred into micelles can be described as the end of micellization temperature (T_{end}). In SAXS profiles, T_{end} can be identified as the temperature beyond which there is no further increase of peak intensities (44). As presented, all formulations demonstrated T_{end} in the temperature range of 33-37℃, regardless of their composition, which is in good agreement with the literature (38,44,45).

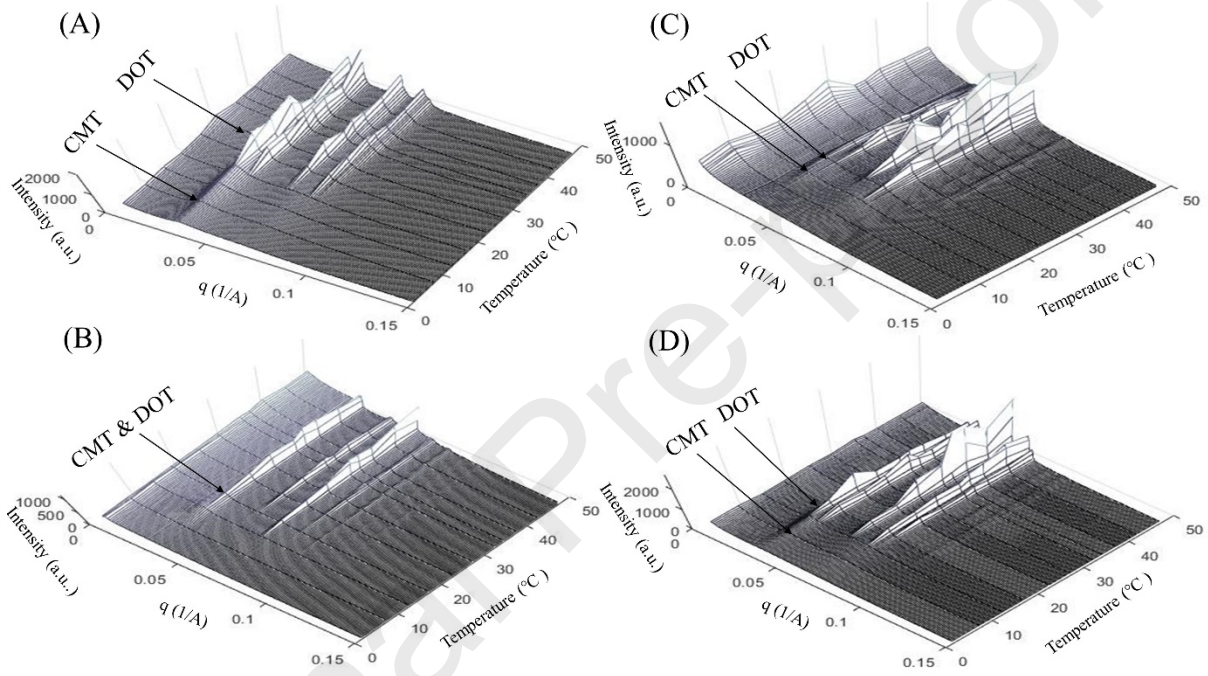

Figure 3: Temperature-dependent structure formation in BH/KT loaded formulations of (A) F2, (B) F3, (C) F4 and (D) F3NaCl, showing the influence of matrix composition on the structuring with increasing temperature. CMT represents the critical micellization temperature and is identified by the peak at the lowest q value (first diffraction peak), whereas DOT denotes the temperature at which a transition from disordered to a packed system takes place and is identified by the presence of two or more diffraction peaks.

3.2.2. Supramolecular arrangement

Table 2 shows the relative positions of the scattered peaks recorded at 37℃. As presented, formulations F2, F3 and F3NaCl exhibited scattering at *q* values corresponding to the ratio of 1: √4/3: √8/3: √11/3, denoting a typical face-centered cubic (FCC) arrangement. On the contrary, F4 demonstrated diffraction corresponding to 1, √2, √3, √4, √5, suggesting a body-centered cubic (BCC) arrangement. Generally, blending of poloxamers of relatively lower PPO/PEO ratios into P407 solution could modify the lattice arrangement, with a potential impact on the release profile (46–48). Further studies are required to identify whether the

change in lattice arrangement is attributed to the change of PPO/PEO ratio and/ or the increased concentration. Of note, inclusion of NaCl into the poloxamer mixture (F3NaCl), did not alter the lattice arrangement compared to F3, implying that sodium/poloxamer interactions are limited to the micellar corona.

Though the loading of BH and KT into poloxamers induced a slight positive shift of the first diffraction peak (q_{1st}), it didn't alter the supramolecular arrangement. The minimal influence of BH/KT on the supramolecular arrangement might be attributed to their high aqueous solubility (11,14), suggesting their existence in the intermicellar aqueous channels without interference with the micellar arrangement (21). The small shift of the signal at low q value might indicate a possible interaction at the interface with the micellar corona, causing a slight increase in micellar diameter (37,48).

Study of the lattice parameters is a key element to understand formulation performance, as drug diffusion is the dominant release mechanism of small hydrophilic drugs (18). As presented in Table 2, the system porosity, denoted by the distance between adjacent micellar layers, decreases by increasing poloxamer concentration, suggesting an increase in micellar diameter as a function of poloxamer concentration. Therefore, increasing the concentration of the poloxamers decreases the system porosity, with a potential to reduce drug diffusion rates and sustain its release.

Table 2: Relative peak position and molecular arrangement of BH/KT loaded formulations at 37℃, showing the influence of matrix composition on the supramolecular arrangement. Lattice was assigned according to (27).

Formulation code	Peaks positions (q)	Relative positions (q_{nth}/q_{1st})	Supramolecular arrangement	d* (A)
F2	0.0398, 0.0450, 0.0647, 0.0759, 0.0810	1, √4/3, √8/3, √11/3, √12/3	Face-centered cubic	83.7
F3	0.0378, 0.0433, 0.0724, 0.0750	1, √4/3, √8/3, √11/3, √12/3	Face-centered cubic	65.7
F4	0.0398, 0.0561, 0.0690, 0.0802, 0.0890	1, √2, √3, √4, √5	Body-centered cubic	59.3
F3NaCl	0.0378, 0.0433, 0.0724, 0.0750	1, √4/3, √8/3, √11/3, √12/3	Face-centered cubic	65.7

*: d= 2π/q; where d is the distance between two adjacent planes (layers), and the q_{ist} is the position of the first diffraction peak with lowest q value (49).

3.3. Interaction and chemical compatibility between formulation components

3.3.1. Fourier transform infra-red (FTIR) spectroscopy

Probing the intermolecular interactions between various formulation components is critical to ensure their chemical compatibility (50). As presented in Figure 4, the inclusion of BH, KT or NaCl, individually, into poloxamers solution triggered a shifting of their characteristic peaks, denoting intermolecular interactions between poloxamers and added materials. Yet, all characteristic peaks were preserved, suggesting the chemical compatibility between various formulation components.

The inclusion of BH into poloxamer solution caused a shift of the peak corresponding to poloxamer ethereal oxygen (C-O-C) stretching from 1099.3 to 1103.2 cm^{-1}. On the other hand, BH spectrum exhibited a shift in its secondary amine group (C-N) stretching from 3240.2 to 3244.1 cm^{-1} and the amide carbonyl group (NC=O) stretching peak split from a doublet to a triplet peak. These results suggest a hydrogen bonding between the electronegative ethereal oxygen (C-O-C) of poloxamer and amine and amide groups of BH, where nitrogen can act as a proton donor (23). Likewise, the inclusion of KT into poloxamer solution caused a blue shift of the ethereal oxygen (C-O-C) stretching peak from 1099.3 to 1101.3 cm^{-1}, whereas KT demonstrated a shift in its amine (N-H) stretching from 3344.3 to 3343.5 cm^{-1}, suggesting a mild interaction between them. Likewise, the blending of NaCl with poloxamer solution caused a shift of its ethereal oxygen transmittance (C-O-C) from 1099.3 to 1103.2 cm^{-1}, and C-H alkane from 1359.7 to 1348.1 cm^{-1}, attributed to the strong ionic crosslinking between sodium cations and poloxamers (33,34).

To investigate the chemical compatibility between KT and BH, the FTIR spectrum of their mixture was compared to their individual spectra. KT exhibited a shift of its N-H stretching from 3344.3 to 3342.8 cm^{-1}, whereas BH showed a red shift of its hydroxyl group (O-H) from 3508.4 to 3506.4 cm^{-1} and amide carbonyl C=O stretching from 1654.8 to 1652.9 cm^{-1}, suggesting a hydrogen bonding between the amine group of KT and the hydroxyl and amide carbonyl functional groups of BH. Likewise, N-H stretching of BH shifted from 3236.4 to 3330.9 cm^{-1}, which could be attributed to the hydrogen bonding between BH amine group and the free hydroxyl of KT.

The FTIR spectrum recorded for poloxamer formulation containing both BH and KT drugs demonstrated mild changes, as compared to their individual spectra. However, the characteristic absorption bands are retained, suggesting that the chemical entity of the three components is preserved. Of note, the recorded intermolecular interactions between poloxamers and other formulation ingredients may contribute to the observed variation in the

sol-to-gel transition temperature between blank and drug-loaded formulations. More importantly, they are likely to reduce the rate of BH/KT diffusion and sustain their release profile (18).

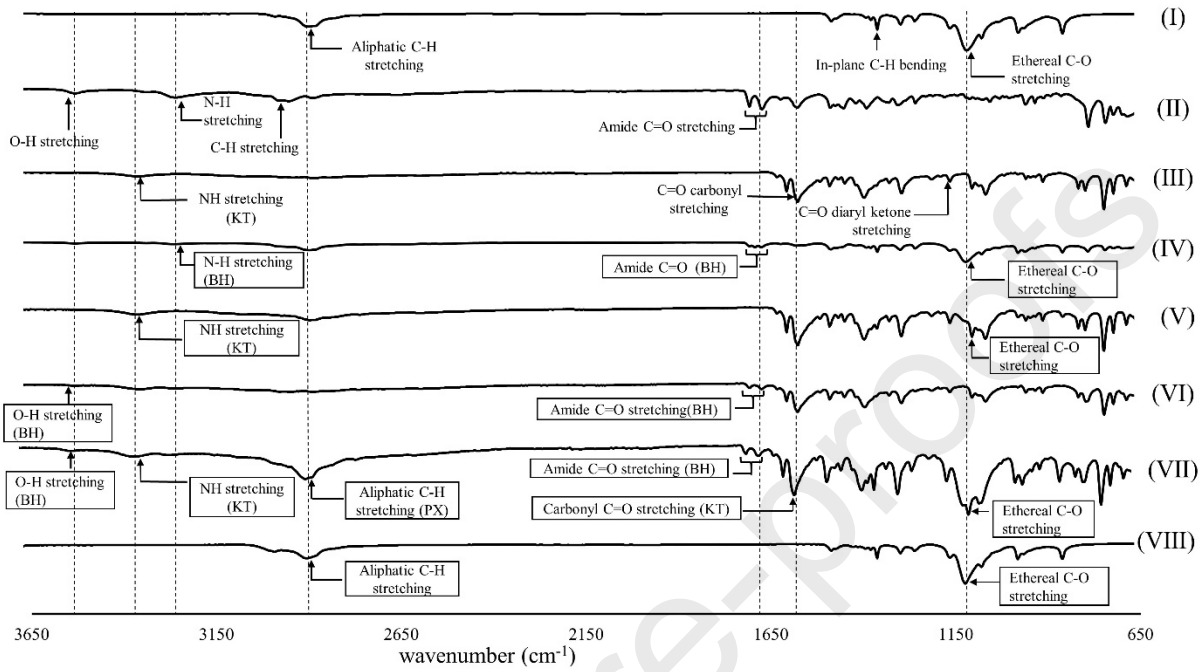

Figure 4: FTIR spectra of (Ⅰ) poloxamers, (Ⅱ) bupivacaine hydrochloride (BH), (Ⅲ) ketorolac tromethamine (KT), (Ⅳ) poloxamer: BH (1:1 mixture), (Ⅴ) poloxamer:KT (1:1 mixture), (Ⅵ) BH:KT (1:1 mixture), (Ⅶ) poloxamer: BH: KT (1:1:1 mixture) and (Ⅷ) poloxamer: sodium chloride (1:1 mixture). Shifted peaks are indicated with vertical dotted lines and outlined text boxes.

3.3.2. Differential scanning calorimetry (DSC) studies

To further assess the compatibility among various components of the developed *in-situ* gels, thermal analysis was performed. In agreement with FTIR findings, the obtained results suggested intermolecular interactions between loaded drugs and poloxamers (Figure 5).

As presented, poloxamers (1:4 mixture of P407 and P188) exhibited a single endothermic peak at 55.3℃, attributed to their melting phenomenon, which is in good agreement with the literature (51,52). DSC curve of BH showed two endothermic peaks at 111.4 and 255℃, corresponding to the loss of water of crystallization and melting, respectively (53–55). On the other hand, the DSC traces of their mixture demonstrated a slight reduction in poloxamers melting temperature to 53.5℃, whereas BH demonstrated a doublet melting peak. The change in BH melting peak shape could be attributed to the formation of various crystal forms since poloxamers melt at a significantly lower temperature than BH, which could affect the heat transfer rate and melting kinetics (52,55).

In agreement with the literature, KT exhibited a sharp characteristic endothermic peak at 165.3℃, attributed to its melting temperature (56,57). Mixing of poloxamers and KT resulted in reducing their melting temperatures to 50.4 and 134.3℃, respectively. This could be attributed to ionic interactions between poloxamers and KT, as suggested by FTIR findings. On the contrary, no changes of poloxamers melting point were observed following NaCl inclusion. Notably, blending of BH and KT caused a drop of KT melting temperature from 165.3 to 147.3℃, whereas BH demonstrated a broad endothermic peak at 248.5℃ corresponding to its melting, suggesting an intermolecular interaction between KT and BH as demonstrated by FTIR findings.

The DSC curve of poloxamers-BH/KT mixture exhibited three endothermic peaks at 53.5, 139 and 258.3℃, attributed to the melting of poloxamers, KT and BH, respectively, suggesting intermolecular interactions between the two drugs with no evidence of incompatibility, which is in agreement with FTIR results.

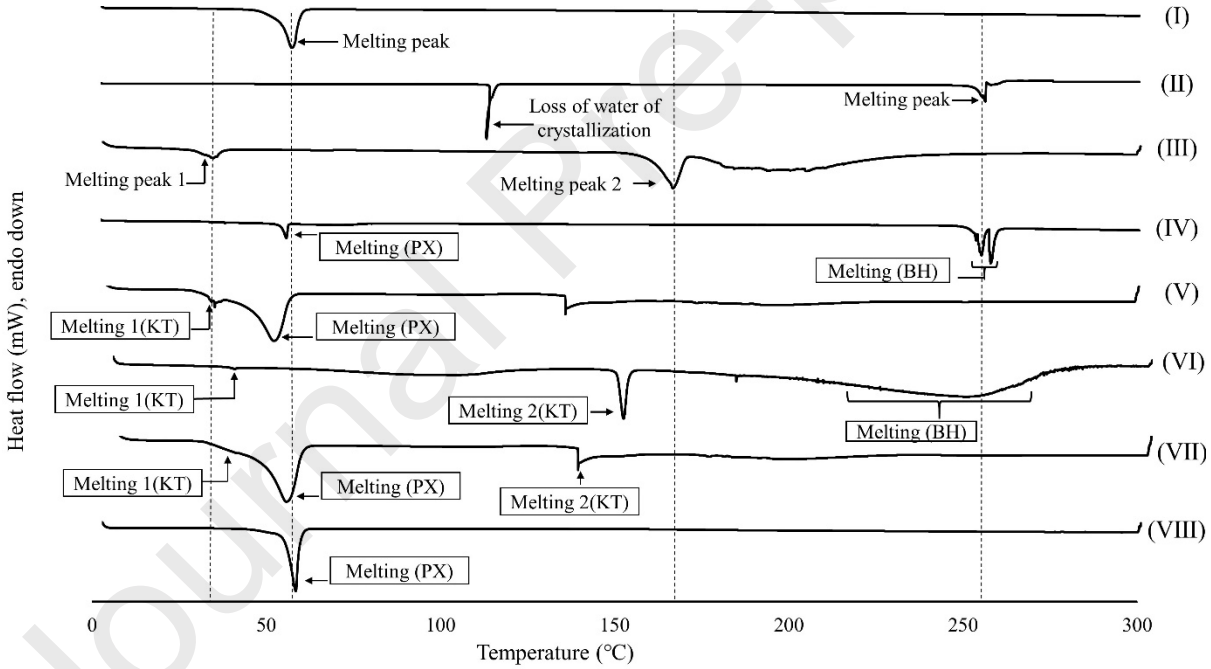

Figure 5: DSC curves of (Ⅰ) poloxamers, (Ⅱ) bupivacaine hydrochloride (BH), (Ⅲ) ketorolac tromethamine (KT), (Ⅳ) poloxamer: BH (1:1 mixture), (Ⅴ) poloxamer:KT (1:1 mixture), (Ⅵ) BH:KT (1:1 mixture), (Ⅶ) poloxamer: BH: KT (1:1:1 mixture) and (Ⅷ) poloxamer: sodium chloride (1:1 mixture). All curves were recorded for freeze-dried powders. Shifted peaks are indicated with vertical dotted lines and outlined boxes.

3.4. Mechanical properties

3.4.1. Gel strength and hardness

The mechanical properties of the formulations are shown in Table 3. As presented, a direct relationship was observed between total poloxamer concentration and gel strength/hardness. Formulations F2 and F3 exhibited significantly higher gel strength ($P < 0.0001$ and 0.05 respectively) and hardness ($P < 0.0005$ and 0.05 respectively), as compared to F4. This observation corroborates the SAXS findings, which demonstrated that increasing the poloxamer concentration reduced the porosity of the system, promoting the micellar entanglement and thus leading to increased gel strength. In agreement with the literature, inclusion of NaCl into poloxamers (F3NaCl), significantly promoted the gel strength ($P < 0.005$) and hardness ($P < 0.05$), as compared to F3 (33,58), attributed to the salting out effect and crosslinking between sodium ions and poloxamers as demonstrated by FTIR.

The gel strength by penetration represents the force required to rupture the internal structure and it provides information on the system compactness. In comparison, the gel hardness is a measure of the gel strength under compression/deformation (59). Both the gel strength and hardness play a crucial role in predicting the *in vivo* performance of poloxamer-based *in-situ* gels. A formulation with high gel strength, such as F2, is likely to maintain its *in vivo* integrity for a longer duration with a potential to sustain drug release, wherever gel erosion is the rate limiting step (18). However, attention is required in the development of injectables, since increasing poloxamer concentration may enhance the formulation viscosity, creating higher resistance for syringeability/injectability.

3.4.2. Injectability

The total work and maximum force required for injectability are shown in Table 3. In agreement with gel strength/hardness data, F2 exhibited significantly higher resistance to injectability ($P <0.005$), attributed to its higher viscosity as demonstrated under rheological analysis (section 3.5.1). Likewise, F3NaCl demonstrated significantly higher resistance to injectability ($P <0.05$) compared to F3. Of note, the injectability of F4 was not assessed as the formulation turned into a gel at the test temperature. Though there are no official limits described, it is recommended that the maximum force required for injection should not exceed 3000 g for the ease of manual injection (60), suggesting the suitability of the developed formulations (except F4) for the intended purpose.

Table 3: Gel hardness and strength at 37℃ and injectability data (represented as maximum force and work done) at ambient room temperature (20℃), showing that increasing poloxamer concentration and inclusion of NaCl promoted the gel mechanical properties (n=3 ± s.d.).

Formulation code	Gel hardness (g) Mean ± SD	Gel strength (g. sec) Mean ± SD	Maximum force (g) Mean ± SD	Work (g. meter) Mean ± SD
F2	68.9 ± 4.9	282.4 ± 21.8	2659.9 ± 38.0	54.1 ± 0.5
F3	51.0 ± 3.2	185.8 ±13.4	2108.0 ± 55.6	30.5 ± 1.7
F4	36.7 ± 0.1	143.2 ± 0.4	*	*
F3NaCl	63.9 ± 2.5	231.3 ± 10.3	2289.6 ± 39.8	41.7 ± 0.7

*: Test was not completed, as formulation turned into a gel at test temperature.

3.5. Rheological analysis

3.5.1. Flow sweep and viscosity measurement

The study of apparent viscosity and flow behavior of parenteral formulations is especially important, as they directly affect the ease/difficulty of syringeability and injectability. As presented in Figure 6A, all formulations (except F4), exhibited a Newtonian-like flow at 20℃, suggesting their suitability for injection (61). On the contrary, F4 exhibited pseudoplastic flow attributed to its gel status at test conditions, suggesting its unsuitability for the intended purpose. Of note, increasing the total poloxamer concentration from 28.5% w/w (F3) to 34% w/w (F2) caused a rise of the apparent viscosity independent of the applied stress, attributed to the formation of a more packed and entangled system, as evident from SAXS results (section 3.2.2) (61,62). Likewise, F3NaCl demonstrated higher viscosity compared to F3, attributed to the crosslinking between NaCl and poloxamers that has been shown under FTIR results (section 3.3.1).

Although a formulation with high viscosity is likely to form a stronger gel and contribute to a slower drug release rate, it is challenged by the difficulty of syringeability and injectability (30). It has been postulated that formulations with a viscosity higher than 300 mPas and/or exhibiting shear thickening behavior, are difficult to inject (63).

3.5.2. Linear viscoelastic region

Figure 6B presents the change in moduli strength as a function of oscillation strain amplitude. In agreement with the literature, all formulations demonstrated dominant linear elastic modulus

at low oscillation strain (< 1 to 1.5%), indicating the stability of their internal arrangement over a small range of strain amplitude (64). Above 1.5% amplitude, the developed *in-situ* gels exhibited a progressive decrease in the elastic modulus and increase of the viscous component as a function of oscillation strain, denoting their deformation (64).

The study of the linear viscoelastic region is essential to predict the *in vivo* performance of injectable *in-situ* gels and to better design further rheological characterization. Formulations that can maintain their intrinsic structure under deformation are likely to stay for a longer period of time at the administration site with potential sustained release properties.

3.5.3. Viscoelastic behavior

The analysis of viscoelasticity was conducted at oscillation amplitude below 1%, within the linear viscoelastic region to ensure gel internal structural integrity was maintained. As presented in Figure 6C, all formulations demonstrated dominant elastic properties compared to viscous properties independent of the angular frequency, confirming that all formations exist in the gel status at test conditions. In agreement with the mechanical and other rheological findings, a direct relationship was observed between the poloxamer concentration and elastic modulus. Likewise, the inclusion of NaCl promoted the gel strength, attributed to its crosslinking with poloxamers, as shown by FTIR findings.

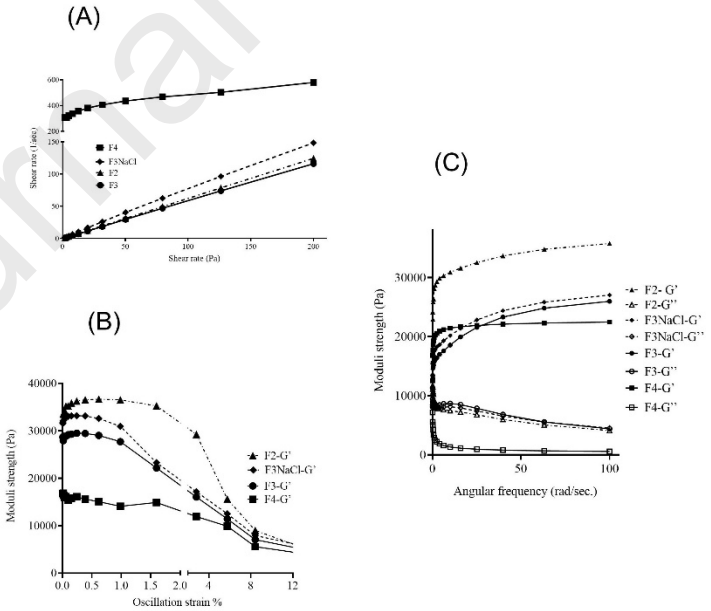

Figure 6: Rheological behavior of the developed formulations. (A) Change of the shear rate as a function of shear stress of BH/KT loaded formulations at 20°C, showing the Newtonian-like flow of F2, F3 and F3NaCl and the pseudoplastic flow of F4, (B) change of formulation moduli strength as a function of strain amplitude, showing

the effect of poloxamer concentration on the gel intrinsic stability and (C) the rheogram of the in-situ gel formulations at 37°C, showing the dominant elastic properties at test conditions.

3.6. *In vitro* drug release

The *in vitro* release profiles of BH and KT from the developed *in-situ* gels are shown in Figures 7A and 7B, respectively. All formulations demonstrated sustained release of both drugs over two weeks. Notably, the percentage cumulative release of BH and KT in the first 6 hours was less than 10% and 8.5%, respectively. An indirect relationship between the total poloxamer concentration and release profile (rate and duration) of BH and KT was observed; F2 exhibited significantly lower release rates $P < 0.05$) compared to F3. The inclusion of NaCl significantly reduced the drug release over the first day ($P < 0.05$). However, after day 1 the release rate was comparable to F3. Kinetic modeling of the release data suggests drug diffusion as the dominant release mechanism for both BH and KT (Table 4). The calculated similarity factors demonstrated the similarity of release profiles of the two drugs (Table 4).

Several attempts have been made to sustain the release of local anesthetics from poloxamer-based *in-situ* gelling systems (21–24). However, these trials were challenged by the short release profile and the initial burst release of the loaded drug. Previous studies have reported a cumulative release of 40-90% of the loaded drug in the first 6 hours (21–24). Here we report less than 10% of cumulative release of both BH and KT in the first 6 hours for all formulations. This could be attributed to the relatively lower sol-to-gel transition temperature and faster gelation, limiting the lag time between injection and phase transition and thus burst release. Reducing the initial burst release carries potential clinical benefits as it may reduce the risk of systemic toxicity (18). In agreement with the SAXS and rheological findings, F3NaCl exhibited limited BH/KT release over the first 6 hours (1.65 and 1.57%, for BH and KT, respectively) attributed to its rapid phase transition.

Although small hydrophilic drugs are likely to diffuse rapidly out of the gel matrix into the surrounding release media, BH and KT demonstrated a sustained release for two weeks. This could be attributed to the highly packed arrangement of the developed matrices, as demonstrated by SAXS, which in turn reduced BH/KT diffusion rates and prolonged their release profiles. In addition, the chemical interactions between BH/KT and poloxamers, as shown by FTIR and thermal analysis, are likely to hinder BH/KT diffusion rates, contributing to the sustained BH/KT release and minimizing the initial burst release (18).The indirect relationship between the total poloxamer concentration and release rates of BH/KT is attributed to the decreased system porosity, as shown by SAXS findings. Formulations with higher

poloxamer concentrations, such as F2, exhibited overall slower drug release, attributed to the relatively smaller intermicellar spaces, which hindered the diffusion of drugs. Besides, the relatively higher gel mechanical and rheological properties demonstrated by F2 are likely to contribute to reduced release rates via slow gel erosion.

The effect of NaCl on the release profiles of the loaded drugs from poloxamer-based *in-situ* gels is debatable in the literature. Several researchers have reported slower release rates of drugs in the presence of NaCl (65–67), whereas others demonstrated that NaCl enhanced the release of meloxicam from poloxamers (34). The present work demonstrates a reduction in the release with the inclusion of NaCl over the first day, followed by slightly higher release rates. The initial reduction of drug release can be attributed to the quick sol-to-gel transition and increased rheological and mechanical properties, which hindered drug diffusion. Thereafter, due to the high water solubility, NaCl tends to diffuse to the bulk solution leaving pores in the gel matrix and enhancing the diffusion of loaded drugs (18,34,66).

Various concentrations of NaCl were initially screened, namely 0.4, 0.6 and 0.9% w/w. It was observed that NaCl enhances the mechanical and rheological properties as a function of its concentration, which is in agreement with the literature (58). Nevertheless, 0.6 and 0.9% w/w NaCl reduced the sol-to-gel transition temperature and the formulations became turbid following storage over a month at 4℃. The formed precipitate was recovered, freeze-dried and analyzed by FTIR. The FTIR data confirmed that the white precipitate is poloxamers, which could be attributed to the salting out effect of NaCl.

Drug release from poloxamers-based *in-situ* gels is controlled by both drug diffusion and gel erosion (68). However, the rate-limiting step varies according to the matrix composition and the physicochemical properties of the loaded drug (69). As shown in Table 4, all formulations demonstrated a greater correlation with the Higuchi kinetic model, suggesting that drug diffusion is the dominant mechanism of release for both BH and KT (21). This could be explained by their hydrophilic nature and small sizes, allowing their diffusion through the interconnected aqueous channels within the gel matrix (21,70,71). This corroborates with the SAXS findings, which demonstrated that BH and KT exist at the interface between polymer chains and aqueous network.

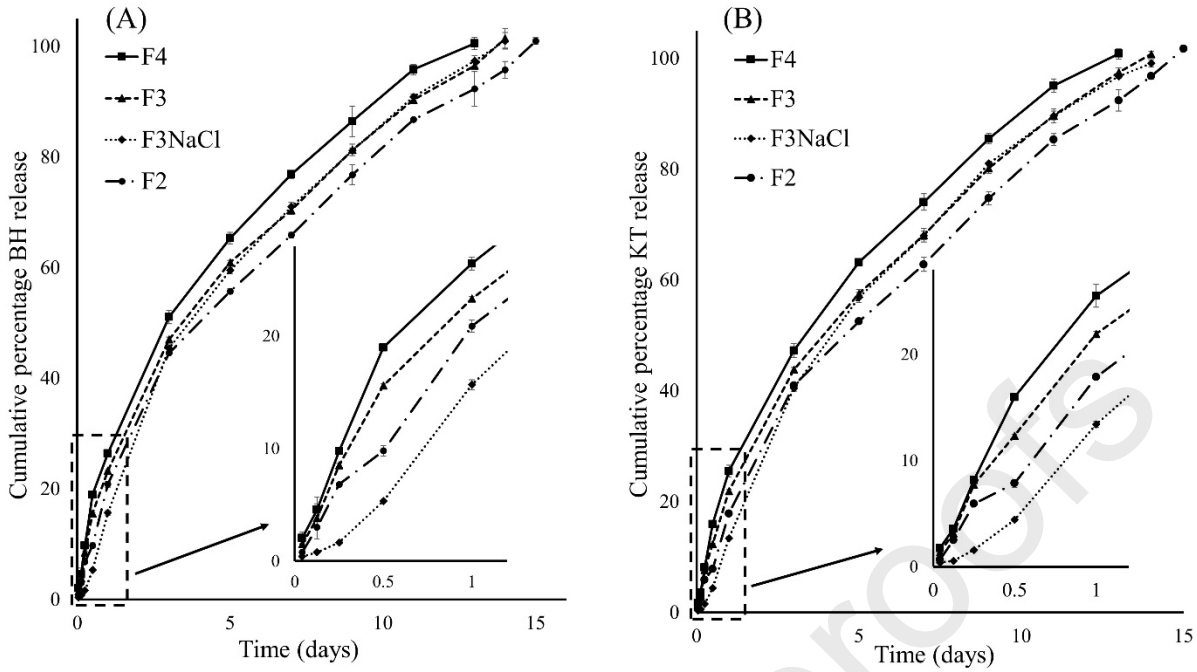

Figure 7: In vitro release profile of (A) bupivacaine hydrochloride and (B) ketorolac tromethamine from test formulations, showing the effect of poloxamer concentration on the drug release profile (n=3). Insets present the release profiles of (A) BH and (B) KT over the first day, showing the limited BH/KT release from F3NaCl, compared to F3.

Table 4: Calculated correlation coefficients of the release data fitting to kinetic models, showing the diffusion as the dominant release mechanism of the developed formulations. The f2 is > 50 for all formulations, suggesting the similarity of release profiles among test formulations.

Formulation code	Zero-order		First-order		Higuchi		Hixson-Crowel		Similarity factor (f2)*	
	BH	KT	BH	KT	BH	KT	BH	KT	BH	KT
F2	0.9516	0.9665	0.8944	0.8216	0.9984	0.9976	0.9801	0.964	55	54
F3	0.9457	0.9579	0.9003	0.8417	0.9990	0.9994	0.9942	0.973	69	69
F4	0.9332	0.9458	0.9588	0.9400	0.9973	0.9990	0.9942	0.9920	NA	NA
F3NaCl	0.9452	0.9556	0.9134	0.9624	0.9943	0.9970	0.9883	0.9942	66	68

*For calculation of f2, formulation F4 was considered as the reference for formulations F2 and F3, whereas the f2 of F3NaCl was calculated against formulation F3.

4. Conclusion

This study is the first to show the development and characterization of an injectable poloxamer-based thermoresponsive *in-situ* forming gels for the simultaneous delivery of bupivacaine hydrochloride and ketorolac tromethamine. The study demonstrated that the sol-to-gel

transition temperature, mechanical and rheological properties of poloxamer-based formulations could be adjusted by modifying the matrix PPO/PEO ratio and/or with the inclusion of salts. SAXS data demonstrated that the intermicellar spacing and supramolecular arrangement could be tailored by modifying the poloxamer ratio and concentration, which in turn influenced drug release rates. Interestingly, the inclusion of sodium chloride significantly reduced the initial burst release from poloxamer-based gelling systems. The findings showed that Fickian diffusion is the prime mechanism of release from the developed poloxamer-based *in-situ* gels for small hydrophilic drugs. This is the first formulation to offer a simultaneous and extended release of BH and KT for up to two weeks and with limited initial burst release, with potential clinical benefits for managing perioperative pain.

Declaration of Competing Interest

The authors declare that they have no known competing financial interests or personal relationships that could have influenced the work reported in this paper.

Funding

This work was supported by the New Zealand Pharmaceutical Education Research Fund [NZPERF] under grant number [3719172].

References

1. Skinner HB. Multimodal acute pain management. Am J Orthop (Belle Mead NJ). 2004 May 1;33(5 Suppl):5–9.

2. Reuben SS, Connelly NR. Postoperative analgesia for outpatient arthroscopic knee surgery with intraarticular bupivacaine and ketorolac. Anesth Analg. 1995;80(6):1154–7.

3. Motififard M, Omidian A, Badiei S. Pre-emptive injection of peri-articular-multimodal drug for post-operative pain management in total knee arthroplasty: a double-blind randomized clinical trial. Int Orthop. 2017 May 1;41(5):939–47.

4. Mahabir RC, Peterson BD, Williamson JS, Valnicek SM, Williamson DG, East WE. Locally administered ketorolac and bupivacaine for control of postoperative pain in breast augmentation patients. Plast Reconstr Surg. 2004 Dec;114(7):1910–6.

5. Arthur GR, Feldman HS, Covino BG. Comparative pharmacokinetics of bupivacaine and ropivacaine, a new amide local anesthetic. Anesth Analg. 1988 Nov 1;67(11):1053–

8.

6. Gaynor JS. Other Drugs Used to Treat Pain. In: Handbook of Veterinary Pain Management. Mosby; 2009. p. 260–76.

7. Gudeman J, Jozwiakowski M, Chollet J, Randell M. Potential risks of pharmacy compounding. Drugs R D. 2013 Mar;13(1):1–8.

8. Becker DE, Reed KL. Local anesthetics: review of pharmacological considerations. Anesth Prog. 2012;59(2):90.

9. Damle Mrinalini C, Deosthali Ajinkya A. Development and validation of HPLC method for determination of modafinil in human plasma. Int J Pharm Technol. 2016;8(2):11932–42.

10. G.Watson D. Pharmaceutical Chemistry E-Book. Churchchil Livingstone Elsevier. 2011.

11. Shah JC, Maniar M. pH-Dependent solubility and dissolution of bupivacaine and its relevance to the formulation of a controlled release system. J Control Release. 1993;23(3):261–70.

12. Calmet J, Esteve C, Boada S, Gine J. Analgesic effect of intra-articular ketorolac in knee arthroscopy: comparison of morphine and bupivacaine. Knee Surgery, Sport Traumatol Arthrosc. 2004 Nov 9;12(6):552–5.

13. Gillis C, Brogden N. Ketorolac. A reappraisal of its pharmacodynamic and pharmacokinetic properties and therapeutic use in pain management. Drugs. 1997;53(1):139–88.

14. Faruki Z, Hossain AKMM, Jha MK, Hasan AKMB. Solubility Enhancement of an Inadequately Water Soluble Drug (Ketorolac Tromethamine) by using different Vehicles. IPP. 2013;1(Dcc):162–71.

15. PubChem. Ketorolac tromethamine. C19H24N2O6 - PubChem [Internet]. 2021 [cited 2021 May 20]. Available from: https://pubchem.ncbi.nlm.nih.gov/compound/Ketorolac-tromethamine

16. DrugBank Online. Ketorolac tromethamine | DrugBank Online [Internet]. [cited 2021 May 20]. Available from: https://go.drugbank.com/salts/DBSALT001045

17. Hersh E V., Dionne RA. Nonopioid Analgesics. In: Pharmacology and Therapeutics for Dentistry: Seventh Edition. Elsevier; 2017. p. 257–75.

18. Abdeltawab H, Svirskis D, Sharma M. Formulation strategies to modulate drug release from poloxamer based in situ gelling systems. Expert Opin Drug Deliv. 2020 Apr 2;17(4):495–509.

19. Haddadi, Hamed. Nazockdast, Ehssan. Ghalei B, Haddadi H, Nazockdast E, Ghalei B, Haddadi, Hamed. Nazockdast, Ehssan. Ghalei B, Haddadi H, et al. Chemorheological Characterization of Thermosetting Polyurethane Formulations Containing Different Chain Extender Contents. Polym Eng Sci. 2008 Dec 1;48(12):2446–53.

20. Larsen C, Ostergaard J, Larsen SW, Jensen H, Jacobsen S, Lindegaard C, et al. Intra-articular depot formulation principles: Role in the management of postoperative pain and arthritic disorders. J Pharm Sci. 2008 Nov;97(11):4622–54.

21. Akkari ACS, Papini JZB, Garcia GK, Franco MKKD, Cavalcanti LP, Gasperini A, et al. Poloxamer 407/188 binary thermosensitive hydrogels as delivery systems for infiltrative local anesthesia: Physico-chemical characterization and pharmacological evaluation. Mater Sci Eng C. 2016 Nov 1;68:299–307.

22. Ricci EJJ, Lunardi LOO, Nanclares DMAMA, Marchetti JMM. Sustained release of lidocaine from Poloxamer 407 gels. Int J Pharm. 2005 Jan 20;288(2):235–44.

23. Sharma M, Chandramouli K, Curley L, Pontre B, Reilly K, Munro J, et al. In vitro and ex vivo characterisation of an in situ gelling formulation for sustained lidocaine release with potential use following knee arthroplasty. Drug Deliv Transl Res. 2018 Jun 6;8(3):820–9.

24. Svirskis D, Chandramouli K, Bhusal P, Wu Z, Alphonso J, Chow J, et al. Injectable thermosensitive gelling delivery system for the sustained release of lidocaine. Ther Deliv. 2016 Jun;7(6):359–68.

25. Sherif AY, Mahrous GM, Alanazi FK. Novel in-situ gel for intravesical administration of ketorolac. Saudi Pharm J. 2018 Sep 1;26(6):845–51.

26. Kirby NM, Mudie ST, Hawley AM, Cookson DJ, Mertens HDT, Cowieson N, et al. A low-background-intensity focusing small-angle X-ray scattering undulator beamline. J Appl Crystallogr. 2013 Dec 1;46(6):1670–80.

27. Hamley IW, Castelletto V. Small-angle scattering of block copolymers in the melt, solution and crystal states. Prog Polym Sci. 2004 Sep;29(9):909–48.

28. Jones DS, Woolfson AD, Brown AF. Textural analysis and flow rheometry of novel, bioadhesive antimicrobial oral gels. Pharm Res. 1997;14(4):450–7.

29. Shavandi A, Bekhit AEDA, Sun Z, Ali MA. Injectable gel from squid pen chitosan for bone tissue engineering applications. J Sol-Gel Sci Technol. 2016 Mar 1;77(3):675–87.

30. Zhang Q, Fassihi MA, Fassihi R. Delivery Considerations of Highly Viscous Polymeric Fluids Mimicking Concentrated Biopharmaceuticals: Assessment of Injectability via Measurement of Total Work Done "W T." AAPS PharmSciTech. 2018 May 1;19(4):1520–8.

31. Hu J, Chen DW, Quan DQ. Rheological properties of poloxamer 407 aqueous solutions. Yaoxue Xuebao. 2011;46(2):227–31.

32. M.A. Fathalla Z, Vangala A, Longman M, Khaled KA, Hussein AK, El-Garhy OH, et al. Poloxamer-based thermoresponsive ketorolac tromethamine in situ gel preparations: Design, characterisation, toxicity and transcorneal permeation studies. Eur J Pharm Biopharm. 2017 May;114:119–34.

33. Choi HG, Lee MK, Kim MH, Kim CK. Effect of additives on the physicochemical properties of liquid suppository bases. Int J Pharm. 1999 Nov 10;190(1):13–9.

34. Inal O, Yapar EA. Effect of mechanical properties on the release of meloxicam from poloxamer gel bases. Indian J Pharm Sci. 2013 Nov;75(6):700–6.

35. Perry HD, Donnenfeld ED. An update on the use of ophthalmic ketorolac tromethamine 0.4%. Expert Opin Pharmacother. 2006 Jan 22;7(1):99–107.

36. dos Santos ACM, Akkari ACS, Ferreira IRS, Maruyama CR, Pascoli M, Guilherme VA, et al. Poloxamer-based binary hydrogels for delivering tramadol hydrochloride: Sol-gel transition studies, dissolution-release kinetics, in vitro toxicity, and pharmacological evaluation. Int J Nanomedicine. 2015 Mar 25;10:2391–401.

37. Valero M, Dreiss CA. Growth, shrinking, and breaking of pluronic micelles in the presence of drugs and/or β-cyclodextrin, a study by small-angle neutron scattering and fluorescence spectroscopy. Langmuir. 2010 Jul 6;26(13):10561–71.

38. LaFollette TA, Walker LM. Structural and mechanical hysteresis at the order-order transition of block copolymer micellar crystals. Polymers (Basel). 2011;3(1):281–98.

39. Hopkins CC, de Bruyn JR. Gelation and long-time relaxation of aqueous solutions of Pluronic F127. J Rheol (N Y N Y). 2019 Jan 8;63(1):191–201.

40. Singh V, Khullar P, Dave PN, Kaur N. Micelles, mixed micelles, and applications of polyoxypropylene (PPO)-polyoxyethylene (PEO)-polyoxypropylene (PPO) triblock polymers. Int J Ind Chem. 2013 Feb 12;4(1):12.

41. Alexandridis P, Alan Hatton T. Poly(ethylene oxide)poly(propylene oxide)poly(ethylene oxide) block copolymer surfactants in aqueous solutions and at interfaces: thermodynamics, structure, dynamics, and modeling. Colloids Surfaces A Physicochem Eng Asp. 1995;96(1–2):1–46.

42. Desai M, Jain NJ, Sharma R, Bahadur P. Temperature and salt-induced micellization of some block copolymers in aqueous solution. J Surfactants Deterg. 2000;3(2):193–9.

43. Mata JP, Majhi PR, Guo C, Liu HZ, Bahadur P. Concentration, temperature, and salt-induced micellization of a triblock copolymer Pluronic L64 in aqueous media. J Colloid Interface Sci. 2005 Dec 15;292(2):548–56.

44. Artzner F, Geiger S, Olivier A, Allais C, Finet S, Agnely F. Interactions between poloxamers in aqueous solutions: Micellization and gelation studied by differential scanning calorimetry, small angle X-ray scattering, and rheology. Langmuir. 2007 Apr 24;23(9):5085–92.

45. Brown W, Schillén K, Almgren M, Hvidt S, Bahadur P. Micelle and gel formation in a poly(ethylene oxide)/poly(propylene oxide)/ poly(ethylene oxide) triblock copolymer in water solution. Dynamic and static light scattering and oscillatory shear measurements. J Phys Chem. 1991;95(4):1850–8.

46. Liu T, Chu B. Formation of homogeneous gel-like phases by mixed triblock copolymer micelles in aqueous solution: FCC to BCC phase transition. J Appl Crystallogr. 2000 Jun 1;33(3 I):727–30.

47. McConnell GA, Gast AP, Huang JS, Smith SD. Disorder-order transitions in soft sphere polymer micelles. Phys Rev Lett. 1993 Sep 27;71(13):2102–5.

48. Oshiro A, Da Silva DC, De Mello JC, De Moraes VWR, Cavalcanti LP, Franco MKKD,

et al. Pluronics F-127/l-81 binary hydrogels as drug-delivery systems: Influence of physicochemical aspects on release kinetics and cytotoxicity. Langmuir. 2014 Nov 18;30(45):13689–98.

49. Atkin R, Warr GG. The smallest amphiphiles: Nanostructure in protic room-temperature ionic liquids with short alkyl groups. J Phys Chem B. 2008 Apr 10;112(14):4164–6.

50. Chadha R, Bhandari S. Drug-excipient compatibility screening-Role of thermoanalytical and spectroscopic techniques. Vol. 87, Journal of Pharmaceutical and Biomedical Analysis. Elsevier; 2014. p. 82–97.

51. Nanaki S, Eleftheriou RM, Barmpalexis P, Kostoglou M, Karavas E, Bikiaris D. Evaluation of Dissolution Enhancement of Aprepitant Drug in Ternary Pharmaceutical Solid Dispersions with Soluplus® and Poloxamer 188 Prepared by Melt Mixing. Sci. 2019 Aug 15;1(2):48.

52. Medarević DP, Kachrimanis K, Mitrić M, Djuriš J, Djurić Z, Ibrić S. Dissolution rate enhancement and physicochemical characterization of carbamazepine-poloxamer solid dispersions. Pharm Dev Technol. 2016 Apr 2;21(3):268–76.

53. Jug M, Maestrelli F, Bragagni M, Mura P. Preparation and solid-state characterization of bupivacaine hydrochloride cyclodextrin complexes aimed for buccal delivery. J Pharm Biomed Anal. 2010 May 1;52(1):9–18.

54. Sykuła-Zając A, Łodyga-Chruścińska E, Pałecz B, Dinnebier RE, Griesser UJ, Niederwanger V. Thermal and X-ray analysis of racemic bupivacaine hydrochloride. J Therm Anal Calorim. 2011;105(3):1031–6.

55. Niederwanger V, Gozzo F, Griesser UJ. Characterization of four crystal polymorphs and a monohydrate of s-bupivacaine hydrochloride (levobupivacaine hydrochloride). J Pharm Sci. 2009;98(3):1064–74.

56. Dasankoppa F, Ningangowdar M, Sholapur H. Formulation and evaluation of controlled porosity osmotic pump for oral delivery of ketorolac. J Basic Clin Pharm. 2013;4(1):2.

57. Parthiban KG, Manivannan R, Kumar BS, Ahasan MB. Formulation and evaluation of ketorolac ocular pH-triggered in-situ gel. Int J Drug Dev Res. 2010;2(3):459–67.

58. Yong CS, Choi JS, Quan QZ, Rhee JD, Kim CK, Lim SJ, et al. Effect of sodium chloride on the gelation temperature, gel strength and bioadhesive force of poloxamer gels

containing diclofenac sodium. Int J Pharm. 2001 Sep 11;226(1–2):195–205.

59. Lau MH, Tang J, Paulson AT. Texture profile and turbidity of gellan/gelatin mixed gels. Food Res Int. 2000;33(8):665–71.

60. Burckbuchler V, Mekhloufi G, Giteau AP, Grossiord JL, Huille S, Agnely F. Rheological and syringeability properties of highly concentrated human polyclonal immunoglobulin solutions. Eur J Pharm Biopharm. 2010;76(3):351–6.

61. Fakhari A, Corcoran M, Schwarz A. Thermogelling properties of purified poloxamer 407. Heliyon. 2017 Aug;3(8):e00390.

62. Lin H-RR, Sung KC, Vong W-JJ. In Situ Gelling of Alginate/Pluronic Solutions for Ophthalmic Delivery of Pilocarpine. Biomacromolecules. 2004 Nov;5(6):2358–65.

63. Xuan JJ, Balakrishnan P, Oh DH, Yeo WH, Park SM, Yong CS, et al. Rheological characterization and in vivo evaluation of thermosensitive poloxamer-based hydrogel for intramuscular injection of piroxicam. Int J Pharm. 2010 Aug 16;395(1–2):317–23.

64. Eun-kyoung. Song K-WP. Rheological properties of poloxamer 407 aqueous solutions and gels. Annu Trans Nord Rheol Soc. 2011;19(2):227–31.

65. Yuan Y, Cui Y, Zhang L, Zhu HP, Guo Y-SS, Zhong B, et al. Thermosensitive and mucoadhesive in situ gel based on poloxamer as new carrier for rectal administration of nimesulide. Int J Pharm. 2012 Jul 1;430(1–2):114–9.

66. Park YJ, Yong CS, Kim HM, Rhee JD, Oh YK, Kim CK, et al. Effect of sodium chloride on the release, absorption and safety of diclofenac sodium delivered by poloxamer gel. Int J Pharm. 2003 Sep 16;263(1–2):105–11.

67. Zeng N, Dumortier G, Maury M, Mignet N, Boudy V. Influence of additives on a thermosensitive hydrogel for buccal delivery of salbutamol: Relation between micellization, gelation, mechanic and release properties. Int J Pharm. 2014 Jun 5;467(1–2):70–83.

68. Bodratti AM, Alexandridis P. Formulation of poloxamers for drug delivery. J Funct Biomater. 2018 Jan 18;9(1).

69. Zhang K, Shi X, Lin X, Yao C, Shen L, Feng Y. Poloxamer-based in situ hydrogels for controlled delivery of hydrophilic macromolecules after intramuscular injection in rats.

Drug Deliv. 2015 Apr 3;22(3):375–82.

70. Yang L, Alexandridis P. Controlled Release from Ordered Microstructures Formed by Poloxamer Block Copolymers. In: Controlled Drug Delivery. American Chemical Society (ACS); 2000. p. 364–74.

71. Gilbert JC, Hadgraft J, Bye A, Brookes LG. Drug release from Pluronic F-127 gels. Int J Pharm. 1986 Oct 1;32(2–3):223–8.

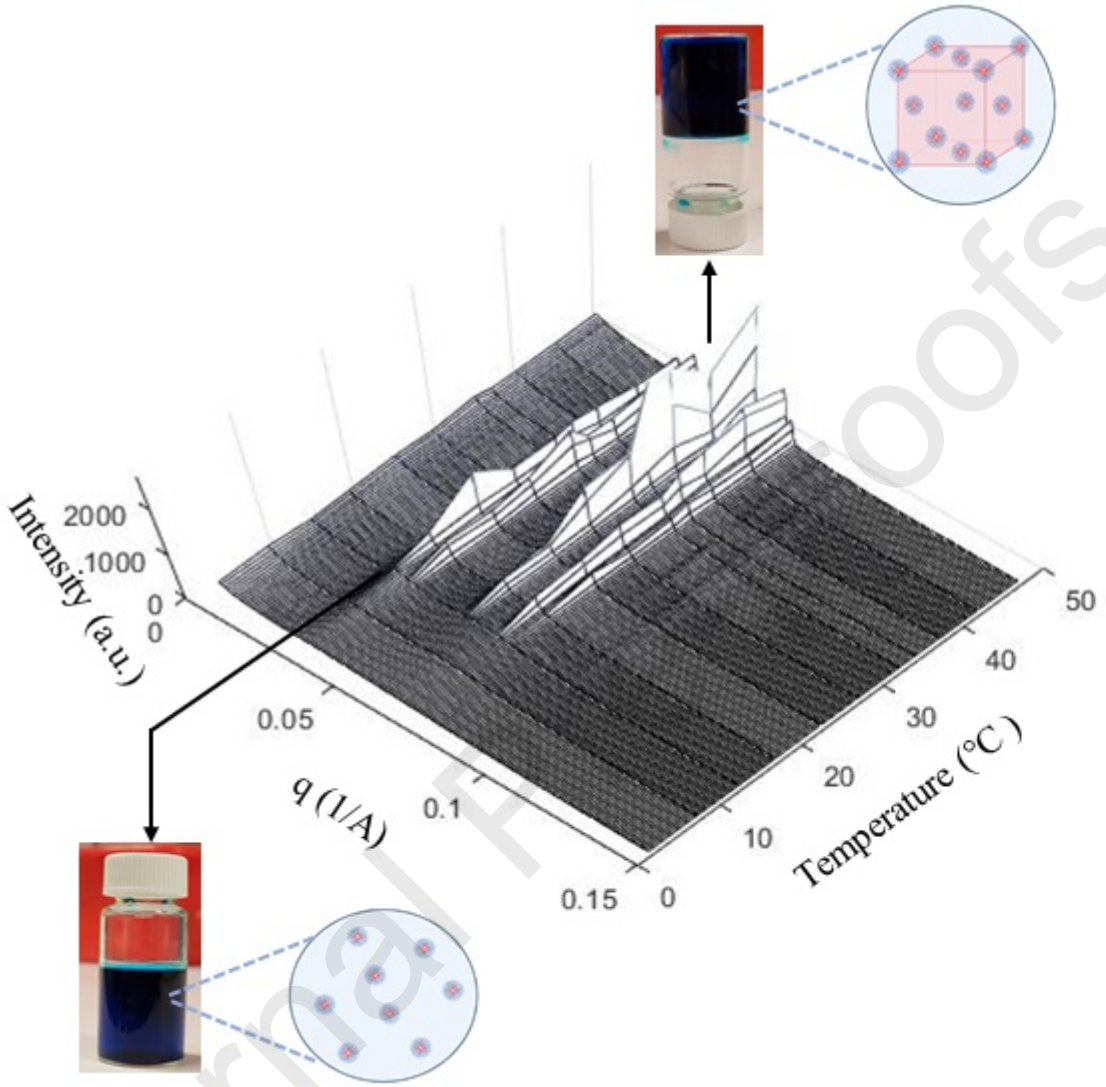

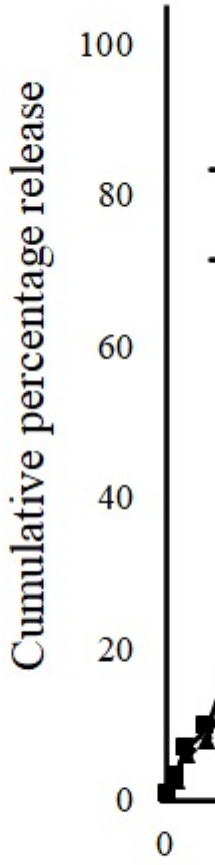

Credit Author Statement:

Hani Abdeltawab: Resources, Methodology, Investigation, Validation, Formal analysis, Writing original draft. **Darren Svirskis**: Conceptualization, Supervision, Funding acquisition, Writing -reviewing and editing. **Ben J Boyd**: Visualization, Methodology, Investigation, Analysis, Writing -reviewing and editing. **Andrew Hill**: Conceptualization, Writing -reviewing and editing. **Manisha Sharma**: Conceptualization, Supervision, Funding acquisition, Project administration, Writing -reviewing and editing. All authors have read and agreed to the published version of the manuscript.

Declaration of interests

☒ The authors declare that they have no known competing financial interests or personal relationships that could have appeared to influence the work reported in this paper.

☐The authors declare the following financial interests/personal relationships which may be considered as potential competing interests: